INT WFS Pipeline Processing

Mike Irwin & Jim Lewis

Institute of Astronomy, Madingley Road, Cambridge

Abstract

We give a brief overview of the INT Wide Field Camera (WFC) together with the automated pipeline processing developed specifically for the Wide Field Survey (WFS). The importance of accurate and complete FITS header information is stresed. Data processing products output from the complete pipeline are discussed.

Key words:
Wide field surveys, automatic processing

1 An overview of the INT WFC

The INT WFC comprises 4 thinned coated EEV 4k × 2k CCDs for the science array plus a thinned 2k × 2k Loral CCD for use as a dedicated frame transfer autoguider. A schematic of the camera layout, with stars from the GSC overlaid, is shown in figure 1 for the default rotator angle of 180 degrees. The inner circle of this figure denotes the 40 arcmin diameter boundary between the unvignetted and vignetted regions, while the dashed outer boundary is the 52 arcmin diameter circle corresponding to 50% vignetting – the practical limit for obtaining viable data. Note that only the top half of the autoguider CCD is active, the bottom half is masked and used as a frame transfer buffer.

The EEV science devices have 13.5 micron pixels corresponding to 0.33 arcsec/pixel at INT prime and each covers an area on sky of 22.8 × 11.4 arcmin. The total sky coverage per exposure for the array is therefore 0.29 square degrees and the total amount of data readout (16-bit pixels) is ≈70 Mbytes per exposure. Current readout time is 160s in the usual readout mode, which in practice leads to a deadtime between exposures of around 3 minutes. Typical observations yield between 5-10 Gbytes of data per night which is archived on single DDS3 DATs for later transfer to Cambridge for pipeline processing.

The Loral autoguider has 15 micron pixels, or 0.37 arcsec/pixel, although

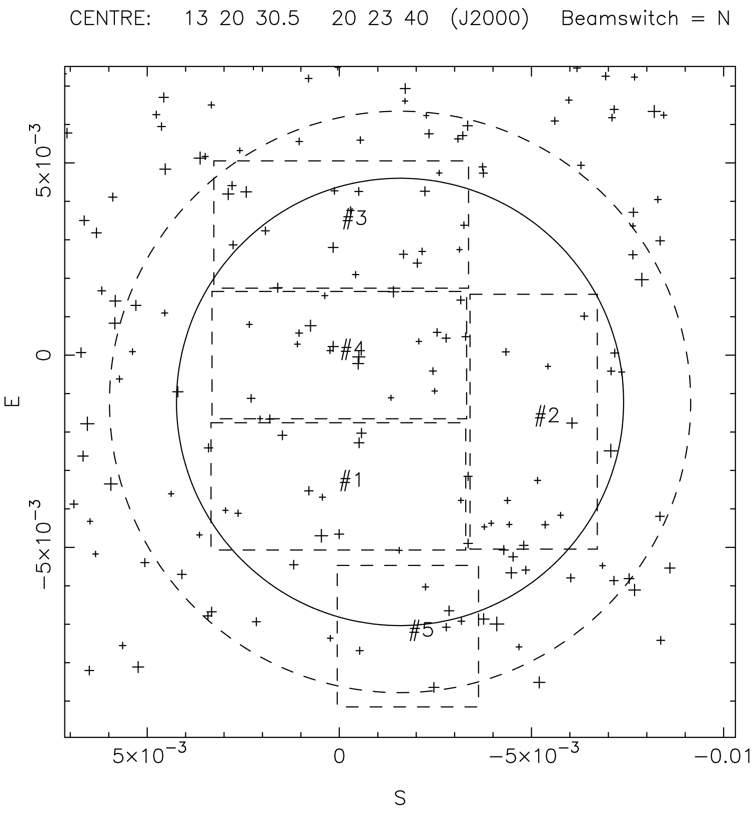

Fig. 1. Overview of the layout of the INT WFC

charge adjacency effects limit the true Loral resolution to 30 microns. The autoguider sees through the same filter as the science devices and is rigidly mounted in the same dewar ensuring that the guiding on the science devices is optimal. The autoguider system uses an APM-style image centroiding algorithm and provides a real-time information display of the guiding status, including: tracking errors, relative transparency and seeing estimates.

A six position filter wheel, holds the 14 cm diameter filters in the f/3 beam, just above the dewar window. Low level N_2 flushing between the filters and the dewar window is used to keep the window moisture-free. Filter changing is automatic and only takes a few seconds. The shutter assembly, a uni-directional circular plate with a contoured aperture, ensures even illumination and is timed by an on-board microprocessor to a few ms. The whole assembly is light tight making sky dawn/dusk flatfielding a practical proposition.

2 INT WFS Pipeline Processing

The amount of data generated during the INT WFS make it impractical to process in an ad hoc manner. We have therefore developed an IRAF-based pipeline to handle the large amounts of data in a mainly automatic way. Although most of the processing is routine and automatic we have found that creating, updating and maintaing master library bias frames, flat-field frames and defringing frames is difficult, if not impossible, to automate in a survey such as this. Since we have no direct control over the observing protocol, a rather varied, set of problems/special cases generally means that we have to interactively construct the master library reference frames for each survey run. Fortunately, given the relatively slow readout speed, we have found that the flat-field frames are stable for periods of around 1 week, the typical survey time allocation slot, and can therefore be constructed from dusk and dawn sky flats.

The data processing pipeline is heavily dependent on the integrity of the FITS header information from the telescope plus instrument and is also used as a repository of information derived and generated by the processing stages. We cannot emphasise enough the vital importance of this information for automated pipeline processing.

The following stages briefly describe the individual tasks carried out during the pipeline processing operations in the order they are applied:

(1) **De-biassing and trimming**
Stacked bias frames using the default clear and readout speeds show some low level repeatable structure due to electronic transient effects, therefore full 2-D bias removal is necessary. All of the requisite debiassing and trimming data and bias sections are specified in the FITS headers.

(2) **Non-linearity correction**
Linearity tests using sequences of dome flats revealed CCD#2 and CCD#4 to have significant, and similar, non-linearities over the whole dynamic range. CCD#1 and CCD#3 are essentially linear to <1% over the full range. A non-linearity correction is applied via a Look Up Table (LUT) to all data. Since CCDs #2 & #4 share one ADC and #1 & #3 another, we believe most of the non-linearity arises in the ADC and should therefore be stable with time.

(3) **Bad pixel replacement**
Bad pixels and dud partial columns are flagged in a master file and are then interpolated over using neighbouring regions.

(4) **Flatfielding**
For each observing run a sequence of master sky flats was constructed. Because of readout overheads it is impossible to generate complete sky flats in, say, UBVRIZ each night, hence flats from several nights are combined to produce master flats. Some low level fringing <0.5% is still visible on the master i', I and Z sky flats but for the current processing we have ignored the slight inaccuracies introduced by this problem.

(5) **Gain correction**

Although processed independently, the mean flatfield sky level in each passband was used to place all the CCDs on the same zeropoint system, ie. sky in deep frames is the same for all CCDs to better than 0.5%, the residual non-linearity level. This step grossly simplies photometric calibration and mosaicing of images.

(6) **Defringing**
Both I and Z-band data frames suffer from significant sky fringes at $\pm 3\%$ and $\pm 6\%$ of sky respectively. R-band images also shows weak fringing at $\pm 0.5\%$ of sky due to the red tail of the Harris glass filter. We find that the SDSS r' filter, because of the well-defined bandpass of 5500 Å– 7000 Å, shows no sky fringing. The SDSS i' filter also has less fringing, $\pm 2\%$ of sky, than the I-band filter, again due to the sharp cutoff at 8500 Å. Fringe patterns in the i', I and particularly Z-band, can show significant variations on a nightly basis, making them difficult to remove completely. We have developed algorithms for automatically removing the sky fringes using fixed fringe pattern masks, that generally reduce the fringing level by a factor of 10 or more. An example of the I-band fringing and its removal for the central region of CCD#1 is shown in figure 2.

(7) **Astrometry**
A zeroth order astrometric World Coordinate System (WCS), accurate to 5–10 arcsec is written to the FITS headers using the nominal telescope pointing, rotator angle and CCD characteristics. Following this, an astrometric solution based on the derived positions of GSC objects visible in the data frames is used to automatically define a more accurate astrometric solution. Currently the external accuracy of this astrometry is limited by the GSC accuracy to about 0.5–1 arcsec. Further improvements of this are underway using deeper Schmidt plate-based astrometry. Preliminary results suggest the final internal astrometric error will be well within 0.1 arcsec for the whole mosaic. The celestial coordinate representation used is based on a polynomial extension of the Zenithal equidistant projection (Greisen & Calabretta 1995).

(8) **Photometry**
A series of selected Landolt standard fields (Landolt 1992) are observed each survey night to monitor and calibrate the photometry to the Johnson-Kron-Cousins photometric system. Colour equations for the INT WFC plus standard filter set are presented elsewhere in this volume. On photometric nights the derived CCD zero-points are consistent to within a few %, assuming an average extinction curve for the site. Current readout time limitations preclude observing sufficient standards to determine the extinction for each night.

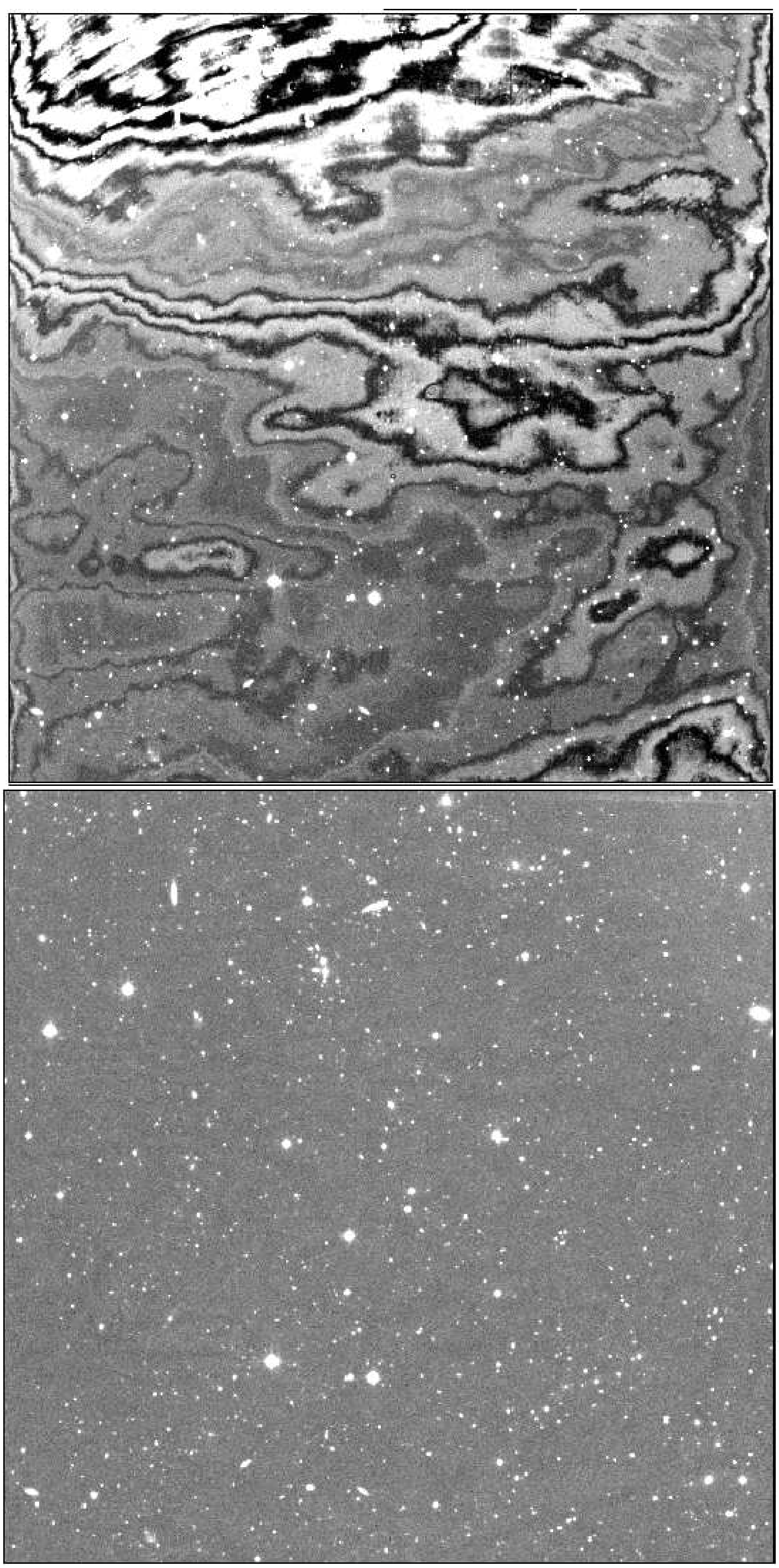

Fig. 2. Fringing in the I-band on CCD#1 before and after automated removal

3 Data Processing Products

The observing logs are automatically generated at the telescope from the FITS headers of the data and provide the reference template for the SYSBASE data archive system. SYSBASE provides a simple user interface to the WFS archive allowing complex querying and data retrieval from the archive. All of the processed WFS data products are stored online, currently using a large disk array to facilitate access to the archive. Future planned upgrades include moving the ever expanding WFS archive to a DVD tower for longer term storage and access. All of the master library bias frames, flatfield frames, and defringing frames plus non-linearity corrections are available via the www and have proven to be a valuable resource for other WFC users.

3.1 Object Catalogues

Each pipeline processed CCD frame is analysed using a standalone automated object detection and parameterisation algorithm based on the ideas presented in Irwin (1985, 1986). Generated parameters include position, intensity and shape information. At the limiting magnitudes reached by the WFS in 10–20 minute integrations ($m_{R} \sim 24$), the majority of the detected images are faint background galaxies. Therefore, to maximise the general usefulness of the catalogues three different types of flux estimates are made:
(i) isophotal – the integrated flux above a specified isophote, ie. the detection isophote of 1.5 σ_n above sky, where σ_n is the pixel-to-pixel noise at sky;
(ii) total – takes the detection isophote for each image and expands it using an elliptical aperture to perform a curve-of-growth analysis (see Hall & MacKay 1984, Irwin 1985, for more details);
(iii) core – this is a "poor man's" PSF fit using a top hat function typically with radius equal to the seeing (FWHM) including sub-pixel integration and simultaneous fitting for blends. It is straightforward to show that for realistic image profiles this flux estimate achieves ~ 0.85 of the signal:to:noise, of the "perfect" PSF fit, but comes at a fraction of the effort. It also works for stars or galaxies.

3.2 Data Quality Control

The software that generates the object catalogues is used to automatically monitor the seeing, sky brightness and noise levels on all the science frames. Examples of the output of this data quality control information are shown in figure 3. These are the fundamental quantities that govern the usefulness of survey data since they determine how deep the survey goes. If we define the

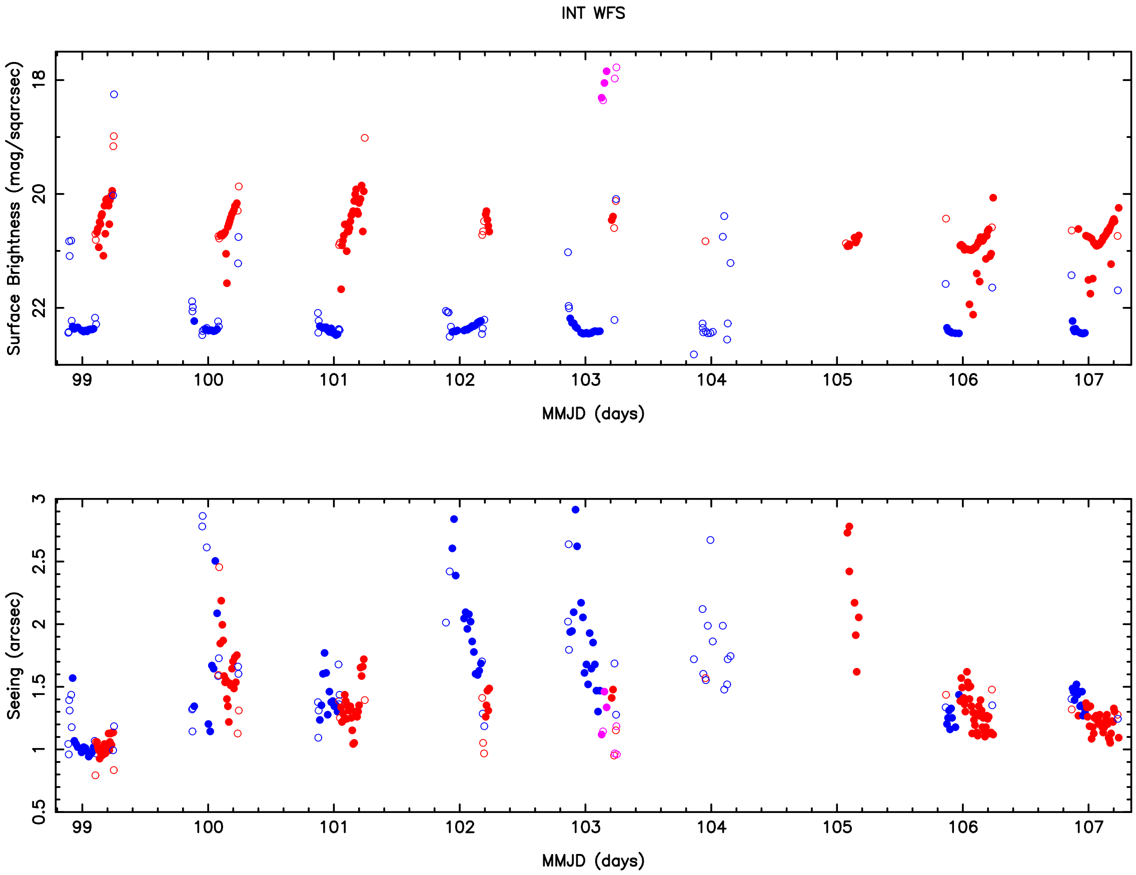

Fig. 3. Sky brightness and seeing estimates for a week of INT WFS data

magnitude limit of a dataset to be that magnitude at which PSF-dominated faint images have a signal:noise of, say, 5:1, then in the absence of confusion limits and using an optimal detection filter, the attainable flux limit is $\propto$ seeing^{-1}. Contrast that with the peak signal:noise which varies as $\propto$ seeing^{-2}. Likewise for sky 1 magnitude brighter than normal, exposures have to be increased by a factor of 2.5 to reach the same limiting magnitude.

References

[1] Greisen, E. W., & Calabretta, M., *Astronomical Data Analysis Software and Systems IV*, ASP Conference Series, Vol. 77, 1995, R.A. Shaw, H.E. Payne, and J.J.E. Hayes, eds., p. 233.

[2] Hall, P., & Mackay, C., 1984 MNRAS, 210, 979.

[3] Irwin, M.J., 1985, MNRAS, 275 514.

[4] Irwin, M.J., 1996, *Instrumentation for Large Telescopes*, VII Canary Islands Winter School, J.M. Rodríguez Espinosa, A. Herrero, F. Sánchez, eds., p. 35.

[5] Landolt, A. U., 1992, AJ, 104, 340.